Xue-Hui Zhan*

Fe-mediated ICAR ATRP of methyl methacrylate on photoinduced miniemulsion polymerization

DOI 10.1515/epoly-2015-0072
Received March 26, 2015; accepted September 12, 2015; previously published online November 19, 2015

Abstract: The initiators for continuous activator regeneration (ICAR) atom transfer radical polymerization (ATRP) of methyl methacrylate (MMA) were investigated in microemulsion under light irradiation with ethyl 2-bromoisbutyrate (EBiB) as an ATRP initiator, ferric chloride hexahydrate ($FeCl_3 \cdot 6H_2O$) as a catalyst, N,N,N′,N′-tetramethyl-1,2-ethanediamine (TMEDA) as a ligand, and azobisisobutyronitrile (AIBN) as an initiator and reducing agent. The linear dependence of $\ln([M]_0/[M])$ on polymerization time was observed, indicating that the polymerization was living polymerization. Furthermore, the number-average molecular weights (Mn), gel permeation chromatography (GPC) and molecular weight distributions (MWD) of the PMMA obtained from GPC were controlled. The product was characterized by ^1H nuclear magnetic resonance (NMR) and GPC. The living features were verified by chain-extended with MMA with the obtained PMMA as macroinitiator.

Keywords: ICAR ATRP; light; living polymerization; methyl methacrylate; miniemulsion.

1 Introduction

Since the introduction of controlled/living radical polymerization (C/LRP), C/LRP has revolutionized the fields of many new advanced materials preparation with a precisely controlled molecular architecture (1–3). The basic conception of CRP is the reversible activation/deactivation of the polymer chains (4). To date, three main living polymerization techniques have been extensively reported: namely nitroxide-mediated radical polymerization (NMP) (5, 6), atom transfer radical polymerization (ATRP) (7–9), reversible addition-fragmentation chain transfer (RAFT) (10–12). Among them, atom transfer radical polymerization (ATRP), also known as metal-mediated radical polymerization, which was independently discovered by Matyjaszewski and Wang (7, 8) and Sawamoto (9) in 1995, is a living radical polymerization that has been attractive in the academic and industrial fields (13, 14). The ATRP technique is a powerful tool for the preparation of (co) polymers with predictable molecular weights and narrow MWD. controlled chain functionality, composition and morphology. In the classic ATRP method, a dynamic exchange amongst the active and the inactive species.

ATRP techniques have been suitable for the polymerization of a wide range of monomers, including styrenes (15, 16), acrylates (17, 18), methacrylates (19, 20), acrylonitrile (21–23) and (meth)acrylamide (24–26). Nevertheless, there are two drawbacks within the conventional ATRP, the first is sensitive to oxygen, which is essential to remove thoroughly the oxygen, the other is higher concentration of catalyst employed. Recently, a new modification of the original ATRP process has been developed by Matyjaszewski and coworkers (27), which was called initiators for continuous activator generation (ICAR) ATRP, In the ICAR ATRP process, a tiny amount of initiator is used to as a reducing agent to generate activators coming from accumulated deactivating species.

Many of the transition metals have been reported in ATRP in complexes of various nitrogen and phosphine-based ligands (28). Copper catalyst is one of the most widely studied transition metal because of its low price, abundant and versatility. Comparing with copper catalyst, iron catalyst is also attractive since its low toxicity, environmentally friendly, biocompatibility, and potential application in biomaterials, and there are many excellent works in the field of iron-catalyzed ATRP reported in ATRP by Zhu and coworkers (29–35).

Miniemulsion polymerization is an ideal method to synthesize nanoscale materials and polymer particles with desirable copolymer composition. The droplets in a miniemulsion are typically between 100 and 500 nm in diameter. In addition, lower viscosity of the medium, polymerization of very hydrophobic monomers, and reduced environmental issues are the general preferences of miniemulsion polymerization. The process of conducting an ATRP in emulsion or miniemulsion provides many advantages and would be an efficient route in commercial production of living free radical polymers. ATRP conducted in

***Corresponding author: Xue-Hui Zhan,** School of Physical and Electron Science, Changsha University of Science and Technology, Changsha 410076, Hunan Province, China,
e-mail:zhanxueh@163.com

miniemulsion or emuclsion has been extensively investigated by the Matyjaszewski group and other groups (36–38). To date, numerous Cu-mediated ATRP performed in miniemulsion have been reported (39, 40). However, only a few reports about iron catalyst have been reported.

There are many potential applications for photoinduced reactions due to no heat needed and good environmental friendly, especially to functional groups and materials that decompose at high temperatures. Photoinduced living polymerizations have been successfully applied to prepare the polymer (41–43). According to our understanding, No reports about photo-induced ATRP in miniemulsion system has been reported.

Herein, we report the preparation of ICAR ATRP of MMA in miniemulsion with ethyl 2-bromoisbutyrate (EBiB) as initiator, $FeCl_3 \cdot 6H_2O$ as catalyst, TMEDA as ligand, and AIBN as initiator and reducing agent. Poly(methyl methacrylate)s (PMMA) with well-defined $M_{n,GPC}$ and narrow MWD were obtained in this system.

2 Experimental

2.1 Materials

MMA was provided by Tianjin Fuchen Chemical Reagents Factory (Tianjin, China) and then distiled under reduced. Ethyl 2-bromoisobutyrate (EBiB, Alfa Aesar Chemical Co., Tianjin, China, 99%) was used directly. AIBN was purchased from Shanghai 4th factory of chemicals, 99%, Shanghai, China) and recrystallized twice from methanol. TMEDA was provided by JinJinLe Industry Co., Ltd. (Shanghai, China). $FeCl_3 \cdot 6H_2O$ was provided by Shanghai Qingfeng Chemical Factory (Shanghai, China). Hexadecane (HD), obtained from Aladdin (Shanghai, China). Polyoxyethylene oleyl ether (brij 98), was purchased from Sinopharm Chemical Reagent (Shanghai, China). The other reagents were used as received.

2.2 Typical procedure for miniemulsion polymerization

The ATRPs were performed according to the following typical procedure. Taking XX as an example, the preparation of organic phase was added hexadecane (HD, 1.8 g, 0.008 mol), AIBN (0.0049 g, 0.00003 mol) and MMA (5 g, 0.05 mol). The composition of aqueous phase consisted of brij 98 (1.5 g, 3 wt.-% vs. monomer), $FeCl_3 \cdot 6H_2O$ (0.0027 g, 0.00001 mol), TMEDA (0.0023 g, 0.00002 mol) in deionized water (30 ml). Then the mixing homogeneous oil phase was placed into the above water phase dropwise with vigorous mechanical agitation for 10 min. Then the initiator EBiB (0.0195 g, 0.0001 mol) was added. The miniemulsion was obtained with sonication at 30 W power (ultrasound cell disruputer, Ninbo Xinzhi Biotech Co.) for 30 min via treatment of the above reaction mixture. The miniemulsion was purged with N_2 for 1 h. Finally, EBiB was added to initiate polymerization. Then the polymerizations were performed under a 500-W, high-pressure mercury vapor lamp, whose distance was about 15 cm at 25°C. At regular intervals, samples were withdrawn with a syringe to measure the conversion, $M_{n,GPC}$ and MWD.

2.3 Chain extension experiment

The Br-terminated polymer was dissolved in MMA (~5 g) in a 150 ml flask. The molar ratio of $[MMA]_0/[PMMA\text{-}Br]_0/[FeCl_3 \cdot 6H_2O]_0/[TMEDA]_0/[AIBN]_0$ was kept 500:1:0.1:0.2:0.3. The flask were irradiated by the light from 500 W high-pressure mercury vapor lamp, whose distance was 15 cm at 25°C. The flask was charged with ultra-high-purity nitrogen for a few minutes. Then it was placed in a oil bath, and the magnetic stirring speed was kept 300 rpm/min. The flask was taken out after light irradiation for some time and cooled to room temperature. After the polymerization was completed, the product was obtained by centrifugation and treated with water and methanol several times, finally dried under vacuum overnight.

2.4 Characterization of PMMA polymer

Monomer conversions were determined gravimetrically. The number-average molecular weights ($M_{n,GPC}$) and molecular weight distribution (MWD) were accessed by Waters 1515 gel permeation chromatography (GPC). The GPC consisted of refractive index detector which was equipped with HR1, HR3, and HR4 column. The eluent was tetrahydrofuran (THF) and the flow rate was 1.0 ml/min and the column teperature was 35°C. Narrowly distributed poly(methyl methacrylate) standards were employed to calibrate the GPC column.

^{1}H NMR spectra were recorded on a Bruker 400 MHz spectrometer with $CDCl_3$ as deuterated solvent. Polymers were dissolved in an appropriate deuterated solvent to give a viscous polymer solution in an NMR tube. The used internal standard was tetramethylsilane (TMS).

3 Results and discussion

3.1 Photoinduced ICAR ATRP of MMA in miniemulsion

The first trial polymerizations for the photo-induced ICAR ATRP of MMA were completed at 25°C in miniemulsion using EBiB/$FeCl_3{\cdot}6H_2O$/TMEDA initiation system. the results were shown in Figure 1 when the molar ratio of $[MMA]_0/[EBiB]_0/[FeCl_3{\cdot}6H_2O]_0/[TMEDA]_0/[AIBN]_0$ was 500:1:0.1:0.2:0.3,

The results shows that the semilogarithmic plot of $\ln[M]_0/[M]$ on time for the ICAR ATRP of MMA in the presence of the $FeCl_3{\cdot}6H_2O$/TMEDA catalyst system is linear. Suggesting constant radical concentration throughout the polymerization process. 76.5% conversion was obtained in miniemulsion within 16 h. The apparent rate constants (k_{app}) obtained from Figure 1 was 2.52×10^{-5} s^{-1}, which is lower than that in bulk and is higher than that in solution polymerization reported by Zhu and coworkers (44). Furthermore, induction period have been observed in above system. It is probably that ICAR ATRP of MMA was performed in different system.

Figure 2 shows the plot of the experimental number average molecular weights ($M_{n,GPC}$) and molecular weight distributions (M_w/M_n) with percentage monomer conversion for the photo-induced ICAR ATRP synthesis of PMMA in miniemulsion. The $M_{n,GPC}$ of the PMMA samples obtained in this systems increased linearly with percentage monomer conversion and are close to the theoretical values ($M_{n,theo}$). The M_w/M_n values are <1.35 during the polymerization process. Based on the above discussion, it can be concluded that the photo-induced ICAR ATRP of MMA was living fashion.

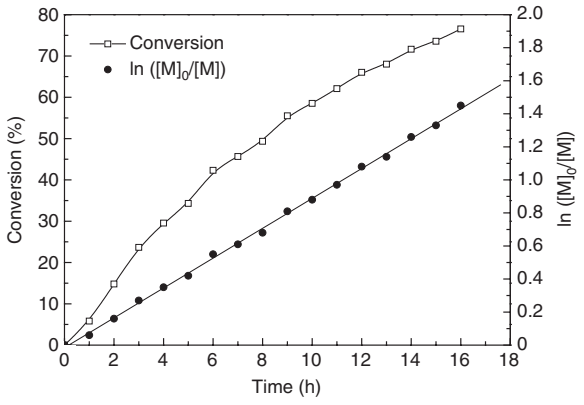

Figure 1: First order kinetics plot of the photoinduced Fe-mediated ICAR ATRP of MMA. Polymerization conditions: $[MMA]_0/[EBiB]_0/[FeCl_3{\cdot}6H_2O]_0/[TMEDA]_0/[AIBN]_0$ was 500:1:0.1:0.2:0.3. Temperature: room temperature. Miniemulsion conditions: $w_{Brij\ 98}$=1.5 g, w_{HD}=1.8 g.

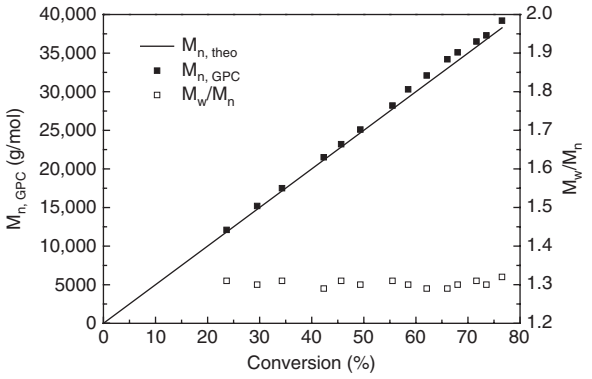

Figure 2: Plots of $M_{n,GPC}$ and molecular weight distribution (MWD) versus percentage monomer conversion for the photoinduced Fe-mediated ICAR ATRP of MMA at 25°C in miniemulsion. The polymerization conditions were the same as Figure 1.

3.2 Effect of molar ratio of $[FeCl_3{\cdot}6H_2O]/[AIBN]$ on photo-induced ICAR ATRP of MMA

In a typical ICAR ATRP system, the molar ratio of $[FeCl_3{\cdot}6H_2O]/[AIBN]$ exerts a vital role in ICAR ATRP. The activators (lower oxidation state transition metals) are continuously generated by in-situ reduction between the deactivators (higher oxidation state transition metal) and the conventional thermal radical initiator (such as azobis(isobutyronitrile) (AIBN)). A serials of experiments were performed at 25°C in order to investigate the effect of $[FeCl_3{\cdot}6H_2O]/[AIBN]$ on photo-induced Fe-mediated ICAR ATRP in miniemulsion. The molar ratio of $[MMA]_0/[EBiB]_0$ was kept 500:1 with varied molar ratios of $[FeCl_3{\cdot}6H_2O]_0/[AIBN]_0$. The results were listed in Table 1.

Seen from Table 1, the conversion increased from 18.4% to 51.3% when the molar ratio of $[FeCl_3{\cdot}6H_2O]_0/[AIBN]_0$ changed from 0.01:0.3 to 0.3:0.3. The $M_{n,GPC}$ of the resulting PMMA were in good agreement with the theoretical values. Furthermore, the M_w/M_n values were <1.35, which indicated that the photoinduced ICAR ATRP of MMA proceeded in a living fashion in miniemulsion. However, the M_w/M_n value was beyond 1.5 when the molar ratio of $[FeCl_3{\cdot}6H_2O]_0/[AIBN]_0$ was 0.005:0.3, indicating that the polymerization was out of control.

3.3 Effect of concentration of $FeCl_3{\cdot}6H_2O$ on photo-induced ICAR ATRP of MMA

The advantage of ICAR ATRP over AGET ATRP is that less amount of catalyst is needed. Thus, the minimum concentration of $FeCl_3{\cdot}6H_2O$ required to be determined. The results are shown in Table 2.

Table 1: Effect of the molar ratio of $[FeCl_3{\cdot}6H_2O]_0/[AIBN]_0$ on photoinduced Fe-mediated ICAR ATRP at 25°C[a].

Run	R[b]	Time (h)	Conversion (%)	$M_{n,theo}$ (g·mol^{-1})	$M_{n,GPC}$ (g·mol^{-1})	M_w/M_n
1[c]	500:1:0.005:0.01:0.3	7	18.4	9175	11,200	1.54
2[c]	500:1:0.01:0.02:0.3	7	28.9	14,430	16,100	1.38
3[c]	500:1:0.05:0.1:0.3	7	36.2	18,120	19,500	1.3
4[c]	500:1:0.1:0.2:0.3	7	45.7	22,830	23,200	1.31
5[c]	500:1:0.3:0.6:0.3	7	51.3	25,630	26,100	1.33

[a]Miniemulsion conditions: $w_{Brij\,98}$=1.5 g, w_{HD}=1.8 g.
[b]R=$[MMA]_0/[EBiB]_0/[FeCl_3{\cdot}6H_2O]_0/[TMEDA]_0/[AIBN]_0$.
[c]The mixtures were irradiated with 500 W high-pressure mercury vapor lamp at a distance of 15 cm at 25°C.

Table 2: Effect of concentration of catalyst on the photoinduced Fe-mediated ICAR ATRP of MMA at 25°C[a].

Run	R[b]	$FeCl_3{\cdot}6H_2O$ (ppm)	Time (h)	Conversion (%)	$M_{n,theo}$ (g·mol^{-1})	$M_{n,GPC}$ (g·mol^{-1})	M_w/M_n
1[c]	500:1:0.05:0.1:0.3	45	10	46.2	23,105	23,800	1.32
2[c]	500:1:0.04:0.1:0.3	36	10	43.9	21,925	22,800	1.35
3[c]	500:1:0.03:0.1:0.3	27	10	41.5	20,760	21,500	1.41
4[c]	500:1:0.02:0.2:0.3	20	10	39.5	19,730	20,600	1.52
5[c]	500:1:0.01:0.3:0.3	9	10	37.3	18,670	19,800	1.65

[a]Miniemulsion conditions: $w_{Brij\,98}$=1.5 g, w_{HD}=1.8 g.
[b]R=$[MMA]_0/[EBiB]_0/[FeCl_3{\cdot}6H_2O]_0/[TMEDA]_0/[AIBN]_0$.
[c]The mixtures were irradiated with 500 W high-pressure mercury vapor lamp at a distance of 15 cm at 25°C.

Table 2 shows the concentration of $FeCl_3{\cdot}6H_2O$ on the photo-induced Fe-mediated ICAR ATRP of MMA in miniemulsion. The concentration of $FeCl_3{\cdot}6H_2O$ changed from 45 ppm to 27 ppm, the polymerization proceeded in a controlled/living process. The number average molecular weights ($M_{n,GPC}$) increased with monomer conversion and were in well agreement with the theoretical values with the molecular weight distribution (M_w/M_n) between 1.32 and 1.41. When the concentration of $FeCl_3{\cdot}6H_2O$ was <20 ppm, the M_w/M_n values became broader indicating out of control of polymerization. This can be attributed to a lower concentration of deactivator and longer transient radical lifetime (45).

3.4 Effect of light irradiance

The light irradiance played an important role in photoinduced polymerization. The effects of light irradiance on photoinduced ICAR ATRP of MMA were also investigated. The light intensity was varied from 20 to 100 W. The molar ratio was kept to be 500:1:0.1:0.2:0.3. The results were shown in Figures 3 and 4.

As shown in Figure 3, first-order kinetics with respect to monomer conversion was linear at different light intensities, indicating that the concentrations of propagating radical are almost constant throughout the polymerization. However, the induction periods were observed in all cases with different light intensities 100 W, 50 W and 20 W used, respectively. At higher irradiance, the induction period became shorter because the generation of more initiating radicals can be generated. Furthermore, 69.3% was reached within 30 h at 100 W and 33.6% was reached within 30 h at 20 W. The apparent rate constant (k_{app}) obtained from Figure 3 were, 1.16×10^{-5} s^{-1}, 7.20×10^{-6} s^{-1} and 4.39×10^{-6} s^{-1}, respectively.

The evolution of $M_{n,GPC}$ and MWD with conversion for the photo-induced ICAR ATRP of MMA at different light intensities were investigated. $M_{n,GPC}$ increased linearly with monomer conversion in all experiments as seen from Figure 4, $M_{n,GPC}$ values were close to the theoretical values when higher light intensities were employed. However, when lower light intensities were employed, the $M_{n,GPC}$ values are slightly higher than the theoretical values. The M_w/M_n values of PMMA were between 1.29 and 1.48. It was further verified that this is sufficiently effective photolysis. It can be conclude that light irradiance had a marked effect on $M_{n,GPC}$ and M_w/M_n values.

3.5 The effect of light on the photoinduced Fe-mediated ICAR ATRP of MMA in miniemulsion

The photo-induced ICAR ATRP of MMA was carried out at 25°C under the conditions of alternating light "ON" and "OFF" environment when keeping $[MMA]_0/$

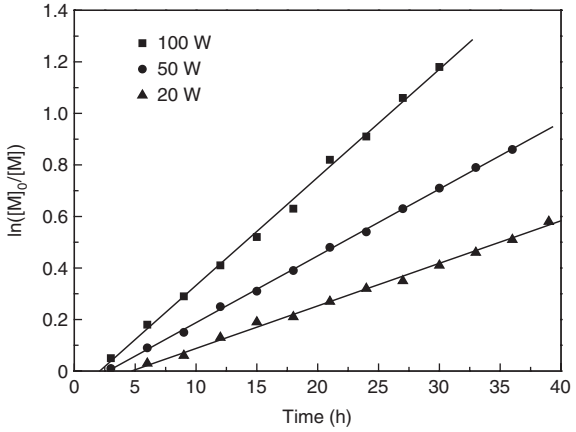

Figure 3: Kinetic plots of photoinduced Fe-mediated ICAR ATRP of MMA at different light intensities at 25°C. Temperature: 25°C. Miniemulsion conditions: $w_{Brij\ 98}$=1.5 g, w_{HD}=1.8 g.

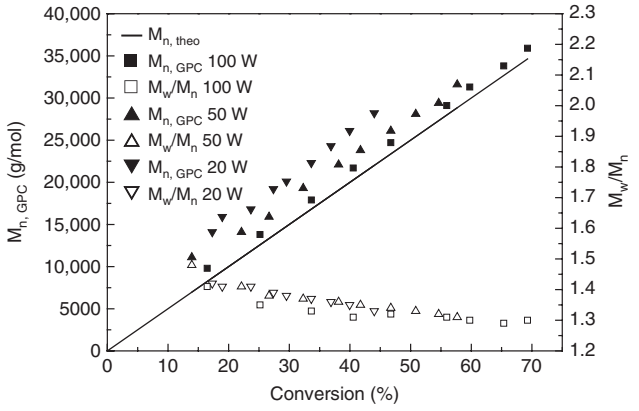

Figure 4: The molecular weight and molecular weight distribution of resulting polymers photoinduced Fe-mediated ICAR ATRP of MMA as a function of conversion. The polymerization conditions were the same as Figure 3.

$[EBiB]_0/[FeCl_3{\cdot}6H_2O]_0/[TMEDA]_0/[AIBN]_0$=500:1:0.1:0.2:0.3, The results were plotted in Figure 5. It can be seen that the initiation period of polymerization was finished when 14.79% conversion was fetched within 2 h under light irradiation and the sufficient radical was obtained. The light irradiation was stopped when irradiation time was in the period of 2–3 h, 4–5 h, 6–7 h, 8–9 h, 10–11 h and 12–13 h.

In addition, it must be demonstrated the polymerization stopped in the absence of light, indicating that the concentration of active species was neglected during the period. However, the polymerization rate increased remarkably in the presence of light. Furthermore, the polymerization rate was the same as the above results mentioned according to the slope. It implied that periodic light on-off process exerted a vital role in this process and demonstrated temporally controlled polymerization.

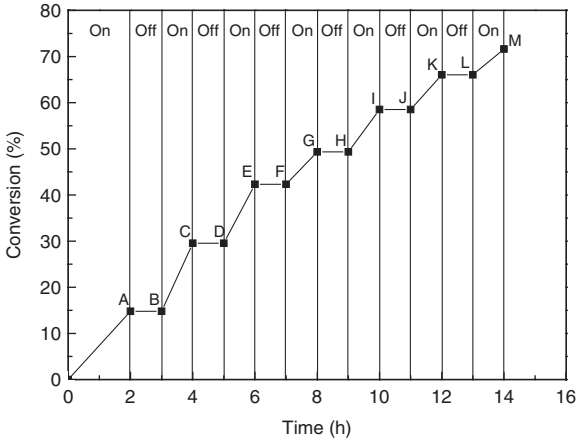

Figure 5: Photoinduced Fe-mediated ICAR ATRP of MMA at 25°C in the presence ("ON") or in the absence ("OFF") of light. Miniemulsion conditions: $w_{Brij\ 98}$=1.5 g, w_{HD}=1.8 g.

Seen from Figure 6, the GPC curves shifted to higher molecule weights in the presence of light. Furthermore, the curves were unimodal, symmetric and relatively narrow (M_w/M_n~1.3) until higher conversion. The GPC curves did almost not shift in the absence of light. These results indicate that the polymerization was controlled by light and the light induces the generation of radicals in miniemulsion.

3.6 Analysis of chain end and chain extension

The PMMA prepared by photo-induced Fe-mediated ICAR ATRP of MMA were also chain extended in miniemulsion using $FeCl_3{\cdot}6H_2O$/TMEDA as the mediator. The mixtures were irradiated with 500 W high-pressure mercury

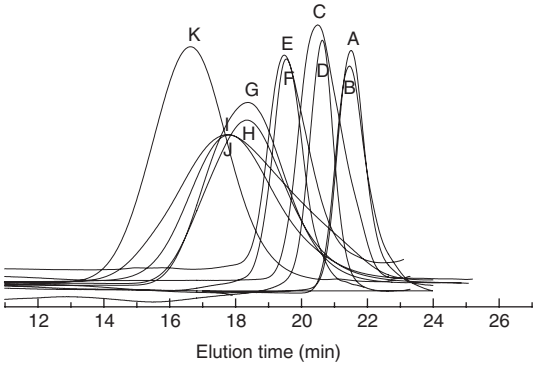

Figure 6: GPC curves of photoinduced Fe-mediated ICAR ATRP of MMA at 25°C. The polymerization conditions were the same as Figure 5.

vapor lamp, whose distance was 15 cm at 25°C. The $[MMA]_0/[PMMA\text{-}Br]_0/[FeCl_3\cdot 6H_2O]_0/[TMEDA]_0/[AIBN]_0$ was 500:1:0.1:0.2:0.3. The macroinitiators was characterized by ^1H NMR spectroscopy (Figure 7). The chemical shift at 0.84–1.21 ppm (a in Figure 7) was contributed to the methyl protons. The shift at 1.42–2.06 ppm (b in Figure 7) was attributed to the protons of methylene groups, 3.41–3.80 ppm (c in Figure 7) was attributed to methoxy groups, 3.78 ppm (d in Figure 7) proved the presence of the end group, as reported by Sawamoto (46). Seen from Figure 8, the $M_{n,GPC}$ of macroinitiators increased significantly from 11,200 g/mol to 283,000 g/mol. MWD of chain-extended PMMA were broad (Figure 8). Active chain end further verified by the successful chain extension in this system.

4 Conclusions

The Fe-mediated ICAR ATRP of MMA using $FeCl_3\cdot 6H_2O$ as catalyst in miniemulsion has been carried out successfully. It was found that the photo-induced ICAR ATRP of MMA obeyed first order kinetics in miniemulsion and the molecular weights increase linearly with the increasing of monomer conversion. The macroinitiator structure was characterized by ^1H NMR spectroscopy and the living nature was verified by chain extension experiment.

Acknowledgments: This work was supported by the National Natural Science Foundation of China (no. 51374043).

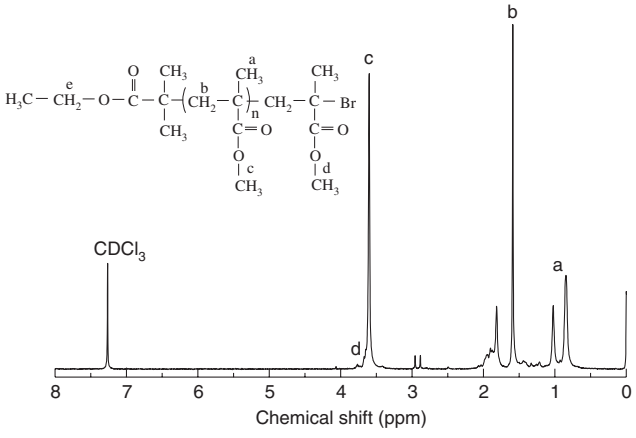

Figure 7: ^1H NMR spectrum of PMMA-Cl.

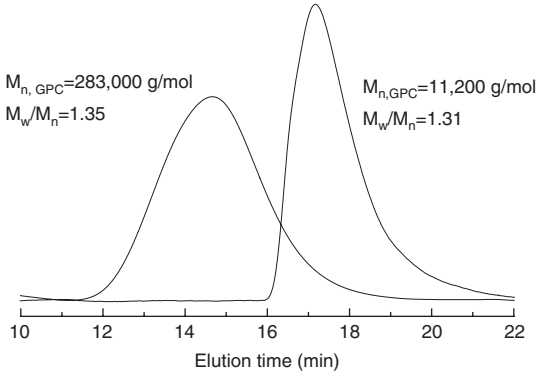

Figure 8: GPC traces of the macroinitiator PMMA-Cl ($M_{n,GPC}$=11,200 g/mol, M_w/M_n=1.31) and the chain extended PMMA ($M_{n,GPC}$=28,300 g/mol, M_w/M_n=1.35).

References

1. Matyjaszewski K. Atom transfer radical polymerization (ATRP): current status and future perspectives. Macromolecules. 2012;45(10):4015–39.
2. Matyjaszewski K, Spanswick J. Controlled/living radical polymerization. Materials Today. 2005;8(3):26–33.
3. Braunecker WA, Matyjaszewski K. Controlled/living radical polymerization: features, developments, and perspectives. Prog Polym Sci. 2007;32(1):93–146.
4. Qiu J, Charleux B, Matyjaszewski K. Controlled/living radical polymerization in aqueous media: homogeneous and heterogeneous systems. Prog Polym Sci. 2001;26(10):2083–134.
5. Georges MK, Veregin RPN, Kazmaier PM, Hamer GK. Narrow molecular weight resins by a free-radical polymerization process. Macromolecules. 1993;26(11):2987–8.
6. Hawker CJ. Molecular weight control by a "living" free-radical polymerization process. J Am Chem Soc. 1994;116(24):11185–6.
7. Wang JS, Matyjaszewski K. Controlled/“living” radical polymerization. Atom transfer radical polymerization in the presence of transition-metal complexes. J Am Chem Soc. 1995;117(20):5614–5.
8. Wang JS, Matyjaszewski K. Controlled/“living” radical polymerization. Halogen atom transfer radical polymerization promoted by a Cu(I)/Cu(II) redox process. Macromolecules. 1995;28(23):7901–10.
9. Kato M, Kamigaito M, Sawamoto M, Higashimura T. Polymerization of methyl methacrylate with the carbon tetrachloride/dichlorotris- (triphenylphosphine)ruthenium(II)/methylaluminum bis(2,6-di-tert-butylphenoxide) initiating system: possibility of living radical polymerization. Macromolecules. 1995;28(5):1721–3.
10. Chiefari J, Chong YK, Ercole F, Krstina J, Jeffrey J, Le TPT, Mayadunne RTA, Meijs GF, Moad CL, Moad G, Rizzardo E, Thang SH. Living free-radical polymerization by reversible addition-fragmentation chain transfer: the RAFT process. Macromolecules. 1998;31(16):5559–62.
11. Diehl C, Laurino P, Azzouz N, Seeberger P H. Accelerated continuous flow RAFT polymerization. Macromolecules. 2010;43(24):10311–4.
12. Keddie DJ, Moad G, Rizzardo E, Thang SH. RAFT agent design and synthesis. Macromolecules. 2012;45(13):5321–42.
13. Pintauer T, Matyjaszewski K. Structural aspects of copper catalyzed atom transfer radical polymerization. Coord Chem Rev. 2005;249(11–12):1155–84.

14. Matyjaszewski K. New materials by atom transfer radical polymerization. Mol Cryst Liq Cryst. 2004;415(1):23–34.
15. Bai LJ, Zhang LF, Zhang ZB, Tu YF, Zhou NC, Cheng ZP, Zhu XL. Iron-mediated AGET ATRP of styrene in the presence of catalytic amounts of base. Macromolecules. 2010;43(22):9283–90.
16. Zhang LF, Cheng ZP, Zhang ZB, Xu DY, Zhu XL. Fe(III)-catalyzed AGET ATRP of styrene using triphenyl phosphine as ligand. Polym Bull. 2010;64(3):233–44.
17. Abreu CMR, Serra AC, Popov AV, Matyjaszewski K, Guliashvili T, Coelho JFJ. Ambient temperature rapid SARA ATRP of acrylates and methacrylates in alcohol-water solutions mediated by a mixed sulfite/Cu(II)Br_2 catalytic system. Polym Chem. 2013;4(23):5629–36.
18. Mendonça PV, Serrab AC, CoelhoJorge FJ, Popov AV, Guliashvilid T. Ambient temperature rapid ATRP of methyl acrylate, methyl methacrylate and styrene in polar solvents with mixed transition metal catalyst system. Eur Polym J. 2011;47(7):1460–6.
19. Magenau AJD, Kwak YW, Matyjaszewski K. ATRP of methacrylates utilizing $Cu^{II}X_2$/L and copper wire. Macromolecules. 2010;43(23):9682–9.
20. Morick J, Buback M, Matyjaszewski K. Effect of pressure on activation-deactivation equilibrium constants for ATRP of methyl methacrylate. Macromol Chem Phys. 2012;213(21):2287–92.
21. Shach-Caplan M, Silverstein M, Bianco-Peled H, Matyjaszewski K. Nanoscale structure of SAN-PEO-SAN triblock copolymers synthesized by atom transfer radical polymerization. Polymer. 2006;47(19):6673–83.
22. Pietrasik J, Dong HC, Matyjaszewski K. Synthesis of high molecular weight poly(styrene-co-acrylonitrile) copolymers with controlled architecture. Macromolecules. 2006;39(19):6384–90.
23. Dong HC, Tang W, Matyjaszewski K. Well-defined high-molecular-weight polyacrylonitrile via activators regenerated by electron transfer ATRP. Macromolecules. 2007;40(9):2974–7.
24. Wever DAZ, Raffam P, Picchioni F, Broekhuis AA. Acrylamide homopolymers and acrylamide-N-isopropylacrylamide block copolymers by atomic transfer radical polymerization in water. Macromolecules. 2012;45(10):4040–5.
25. Jiang JG, Lu XY, Lu Y. Preparation of carboxyl-end-group polyacrylamide with low polydispersity by ATRP initiated with chloroacetic acid. J Polym Sci Part A: Polym Chem. 2007;45(17):3956–65.
26. Jewrajka SK, Mandal BM. Living radical polymerization. II. Improved atom transfer radical polymerization of acrylamide in aqueous glycerol media with a novel pentamethyldiethylenetriamine-based soluble copper(I) complex catalyst system. J Polym Sci Part A: Polym Chem. 2004;42(10):2483–94.
27. Matyjaszewski K, Jakubowski W, Min K, Tang W, Huang J, Braunecker WA, Tsarevsky NV. Diminishing catalyst concentration in atom transfer radical polymerization with reducing agents. Proc Natl Acad Sci. 2006;103(43):15309–14.
28. Ouchi M, Terashima T, Sawamoto M. Transition metal-catalyzed living radical polymerization: toward perfection in catalysis and precision polymer synthesis. Chem Rev. 2009;109(11):4963–5050.
29. Zhang LF, Miao J, Cheng ZP, Zhu XL. Iron-mediated ICAR ATRP of styrene and methyl methacrylate in the absence of thermal radical initiator. Macromol Rapid Commun. 2010;31(3):275–80.
30. Allan LEN, MacDonald JP, Reckling AM, Kozak CM, Shaver MP. Controlled radical polymerization mediated by amine-bis(phenolate) iron(III) complexes. Macromol Rapid Commun. 2012;33(5):414–8.
31. Xue Z, Nguyen TBL, Noh SK, Lyoo WS. Phosphorus-containing ligands for iron(III)-catalyzed atom transfer radical polymerization. Angew Chem Int Ed. 2008;47(34):6426–9.
32. Zhang L, Cheng Z, Zhang Z, Xu D, Zhu X. Fe(III)-catalyzed AGET ATRP of styrene using triphenyl phosphine as ligand. Polym Bull. 2010;64(3):233–44.
33. Wang Y, Bai L, Chen W, Chen L, Liu Y, Xu T, Cheng Z. Iron-mediated AGET ATRP of MMA using acidic/basic salts as reducing agents. Polym Bull. 2013;70(2):631–42.
34. Liu Y, Xu T, Zhang L, Cheng Z, Zhu X. Bulk AGET ATRP of methyl methacrylate using iron(III) acetylacetonate as a catalyst. Polym Chem. 2014;5(23):6804–10.
35. He W, Cheng L, Zhang L, Liu Z, Cheng Z, Zhu X. A versatile Fe_3O_4 based platform via iron-catalyzed AGET ATRP: towards various multifunctional nanomaterials. Pol Chem. 2014;5(2):638–45.
36. Elsen AM, Burdyńska J, Park S, Matyjaszewski K. Activators regenerated by electron transfer atom transfer radical polymerization in miniemulsion with 50 ppm of copper catalyst. ACS Macro Lett. 2013;2(9):822–5.
37. Elsen AM, Burdynìska J, Park S, Matyjaszewski K. Active ligand for low PPM miniemulsion atom transfer radical polymerization. Macromolecules. 2012;45(18):7356–63.
38. Zhu G, Zhang L, Pan X, Zhang W, Cheng Z, Zhu X. Facile soap-free miniemulsion polymerization of methyl methacrylate via reverse ATRP. Macromol Rapid Commun. 2012;33(24):2121–6.
39. Wang G, Zhu X, Cheng Z, Zhu J. Atom transfer radical polymerization of styrene initiated by the novel initiator 2-bromo-2-nitropropane. e-Polymers. 2005;5(1):357–63.
40. Liu P. Modification of polymeric materials via surface-initiated controlled/"living" radical polymerization. e-Polymers. 2007;7(1):725–55.
41. Xu J, Jung K, Atme A, Shanmugam S, Boyer C. A robust and versatile photoinduced living polymerization of conjugated and unconjugated monomers and its oxygen tolerance. J Am Chem Soc. 2014;136(14):5508–19.
42. Anastasaki A, Nikolaou V, Simula A, Godfrey J, Li M, Nurumbetov G, Wilson P, Haddleton DM. Expanding the scope of the photoinduced living radical polymerization of acrylates in the presence of $CuBr_2$ and Me_6-Tren. Macromolecules. 2014;47(12):3852–9.
43. Zhao Q-L, Liu E-H, Wang G-X, Hou Z-H, Zhan X-H, Liu L-C, Wu H. Photoinduced ICAR ATRP of methyl methacrylate with AIBN as photoinitiator. J Polym Res. 2014;21(5):444–9.
44. Zhu G, Zhang L, Zhang Z, Zhu J, Tu Y, Cheng Z, Zhu X. Iron-mediated ICAR ATRP of methyl methacrylate. Macromolecules, 2011, 44(9):3233–9.
45. Goto A, Fukuda T. Kinetics of living radical polymerization. Prog Polym Sci. 2004;29(4):329–85.
46. Ando T, Kamigaito M, Sawamoto M. Iron(II) chloride complex for living radical polymerization of methyl methacrylate. Macromolecules. 1997;30(16):4507–10.